water

MDPI

Article

Barium-Encapsulated Biodegradable Polycaprolactone for Sulfate Removal

Changseok Han [1,*] and Mallikarjuna N. Nadagouda [2,*]

[1] Department of Environmental Engineering, Inha University, Incheon 22212, Korea
[2] Center for Nanoscale Multifunctional Materials, Mechanical & Material Engineering, Wright State University, Dayton, OH 45431, USA
* Correspondence: hanck@inha.ac.kr (C.H.); nnmalli@yahoo.com (M.N.N.); Tel.: +82-32-860-7505 (C.H.); +1-513-569-7232 (M.N.N.)

Received: 14 September 2018; Accepted: 30 November 2018; Published: 6 December 2018

Abstract: Various compositions of barium carbonate ($BaCO_3$) loaded polycaprolactone (PCL) composites were prepared, including 2.5/97.5, 10/90, 30/70, 50/50 and 90/10 (PCL/$BaCO_3$), via re-precipitation technique. Small-scale column tests were conducted to study the efficiency of sulfate removal using the PCL/$BaCO_3$ composites. The composites before and after their use to remove sulfate were extensively characterized using X-ray diffraction (XRD), scanning electron microscopy (SEM), energy dispersive spectroscopy (EDS), transmission electron microscopy (TEM), high-resolution TEM (HR-TEM), and thermogravimetric analysis (TGA). As PCL is a biodegradable polymer, these composites are environmentally friendly and have several advantages over barium sulfate precipitation in overcoming clogging issues in filters or resins due to collection of natural organic matter (NOM). The media used in this study exhibited high capacity and was able to remove more than 90% sulfate from synthetic sulfate containing waters and NOM samples collected from the Ohio River.

Keywords: barium sulfate; biodegradable polymer; polycaprolactone; environmental remediation; water treatment

1. Introduction

Environmental remediation methods often employ the use of synthetic composites due to their enhanced material properties [1–5]. Sulfate is one of commonly found anions in sources of water supplies, due the presence of atmospheric sulfur dioxide and many high water-soluble minerals containing sulfate, such as sodium sulfate, potassium sulfate, and magnesium sulfate in the environment [6]. Recently, the removal of sulfate from drinking water has been targeted due to deleterious effects of sulfate on the environment [7,8]. Sulfates affect not only the environment but also human health. Abnormal changes resulting from sulfate consumption from drinking water may include diarrhea and dehydration. These ill effects are more prominent during infant years and decline with age [6]. Previously, a novel composite made of polyvinyl chloride (PVC) loaded with barium carbonate ($BaCO_3$) was reported for sulfate removal [9]. The implementation of such a material in a small-scale column test (SST) yielded promising results. However, reports indicate that potential contamination and leaching from conventional plastic like PVC can pose a severe threat to human health and the environment [10,11]. Monomethyl-, dimethyl-, monobutyl-, and dibutyl levels have been found at values up to 291 ng Tin (Sn)/L, 49.1 ng Sn/L, 28.5 ng Sn/L, and 52.3 ng Sn/L, respectively, in drinking water distributed through PVC pipes [12,13]. Successful remediation must involve the reduction of hazardous materials without introducing any further complications. Although the previously synthesized PVC/$BaCO_3$ composite [10] showed promising results, the necessity for a benign and environmentally friendly remediation method still exists [14].

The hydrolytic degradation of several common polyesters has provided an attractive new platform for composite synthesis. In particular, polycaprolactone (PCL) has become a focus of various medical device applications, including drug and bacterial encapsulation [15,16], antimicrobial film development [17], and scaffolding in tissue engineering [18]. PCL exhibits not only significant biocompatibility but also undergoes slow degradation to produce harmless byproducts. Additionally, the glass transition temperature of −60 °C and a low melting temperature near 60 °C result in PCL's substantial amorphous thermoplastic properties. The simple ring-opening polymerization synthesis makes this polymer matrix attractive for nanocomposite formation. PCL shows significant solubility at room temperature in a gamut of solvents, including chloroform, dichloromethane, carbon tetrachloride, benzene, toluene, cyclohexanone, and 2-nitropropane. Such strong properties of PCL make it a suitable alternative to PVC in the previously reported facile synthesis of polymer/$BaCO_3$ composites [7].

In the present work, incorporation of barium into a biodegradable and biocompatible polymer matrix for removal of sulfate from contaminated waters has been investigated. The porous nature of the PCL matrix promotes the use of such a material in column packing applications for environmental remediation. Several issues of previous schemes were addressed in the implementation of PCL. Primarily, hazardous and environmentally damaging PVC was replaced with PCL as a benign matrix. Furthermore, the easily accelerated hydrolytic degradation elucidates a new method for barium sulfate ($BaSO_4$) recovery following its use in the column studies. The resulting PCL and $BaCO_3$ composite (PCL/Ba) showed significant sulfate removal capacity similar to that observed in the previous studies [7]. The process of precipitation is shown in Scheme 1. Concerns of wall effects in column applications were addressed, and the results have been reported in this work.

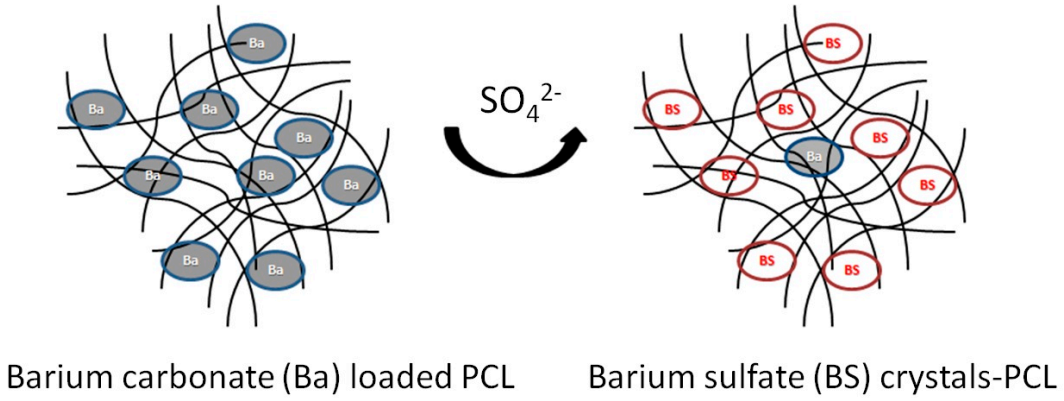

Scheme 1. The phase change from barium carbonate to barium sulfate in the polymer composite on passing sulfate containing water.

2. Experimental Section

2.1. Synthesis of Polymer Composites

Ten grams of PCL (Aldrich; Mn 70–90 kDa) was dissolved in tetrahydrofuran (THF) at 10.0% weight per volume ratio. The solid $BaCO_3$ powder was added to the resulting solution. The heterogeneous mixture was agitated by an IKA Lab Egg compact mixer to create a milky slurry. Subsequently, 100 mL methanol was slowly added to the slurry. Finally, 100 mL of distilled water was added to induce precipitation.

Following the complete addition of water, solid PCL/$BaCO_3$ precipitates settled from the solution to yield a clear supernatant. The composite material was purified by decanting organic solvents and washing three times with distilled water. Various compositions prepared are shown in Table 1.

Table 1. Various PCL/Ba media compositions.

Sample	Composition
PCL/Ba(2.5/97.5)	Polycaprolactone 2.5 wt% + $BaCO_3$ 97.5 wt%
PCL/Ba(10/90)	Polycaprolactone 10 wt% + $BaCO_3$ 90 wt%
PCL/Ba(30/70)	Polycaprolactone 30 wt% + $BaCO_3$ 70 wt%
PCL/Ba(50/50)	Polycaprolactone 50 wt% + $BaCO_3$ 50 wt%
PCL/Ba(90/10)	Polycaprolactone 90 wt% + $BaCO_3$ 10 wt%

2.2. Characterization of PCL/$BaCO_3$ Composites

X-ray diffraction (XRD) patterns were measured using an X'Pert PRO XRD diffractometer (Philips, Almelo, The Netherlands) with Cu K (λ = 1.5406 Å) radiation. To characterize the morphology of PCL/$BaCO_3$ composite samples, an environmental scanning electron microscope (ESEM, Philips XL 30 ESEM-FEG, Eindhoven, The Netherlands) was employed. An energy dispersive spectroscopy (EDS) installed in the ESEM was used to determine Ba content in the samples. A transmission electron microscopy (TEM, Philips CM20, Eindhoven, The Netherlands) and a high resolution-TEM (HR-TEM, JEM-2010F, JEOL, Tokyo, Japan) with a field emission gun at 200 kV were used to investigate the crystal structure and crystal size. Thermogravimetric analysis (TGA) curves were obtained using a Perkin–Elmer Thermal Analyzer with a heating rate of 10 °C/min under air.

2.3. Investigation of the Capacity of PCL/$BaCO_3$ Composites for Sulfate Removal

Column tests were performed to investigate the adsorption capacity of the developed PCL/$BaCO_3$ composite adsorbents for sulfate removal. Two different types of water were tested, one being deionized (DI) water only, and the other containing natural organic matter (NOM). First, sulfate removal using PCL/Ba samples was investigated using clean water without NOM. Sulfate solution of 1100 mg/L was prepared using DI water with a pH of 7.0. The sulfate solution was continuously injected from the top of a column type of reactor. The flow rate of 1 mL/min was kept using a Thermo ScientificTM FH100M Series Peristaltic pump. To investigate the effect of column diameter on the sulfate removal, two reactors with different diameters (i.e., d = 2.25 cm and d = 1.0 cm) were used. Second, to investigate the sulfate removal in the presence of NOM, raw NOM was collected from the Ohio River, Cincinnati, Ohio, USA, which contains sulfate about 100–500 mg/L. Concentrated NOM with a sulfate concentration of 5000 mg/L was diluted to 328 mg/L using DI water and continuously injected into the column type of reactor with a diameter of 2.25 cm. For all experiments, PCL/Ba samples of 1 g were added in the column reactor. The experimental conditions were decided based on the preliminary tests performed at the beginning of this study (not shown). The concentration of sulfate was analyzed using a HACH spectrophotometer (DR 2700) with the USEPA SlulfaVer 4 method, which is equivalent to USEPA method 375.4. The recently updated SlulfaVer 4 method (10th edition, released in February 2018) reported that Ba interferes with sulfate quantification. The maximum error may occur at a concentration about 20% lower than the actual sulfate concentration when Ba concentration is very high.

3. Results and Discussion

XRD analysis was performed to confirm the phase changes from $BaCO_3$ to $BaSO_4$ after sulfate removal. The obtained XRD patterns for PLC/Ba samples before and after sulfate adsorption are shown in Figure 1. All the diffraction peaks were indexed with reference to the unit cell of the barite structure (JCPDS card: 24-1035) or witherite structure (JCPDS card: 00-044-1487). The diffraction peaks of (101), (111), (021), (121), (002), and (212) were characteristic peaks of orthorhombic $BaSO_4$ crystal, demonstrating that the product $BaSO_4$ formed. These results indicate that PCL/Ba samples effectively removed sulfate through the formation of $BaSO_4$. Additionally, these results are in good agreement with a previous report [9], which showed the formation of $BaSO_4$ after sulfate adsorption using $BaCO_3$/PVC composites. However, in the case of the PCL/Ba (50/50) sample, the intensity of

the peak corresponding to barium sulfate is weak due to the presence of increased polymer content that restricts the diffusion of sulfate molecules towards buried barium ions.

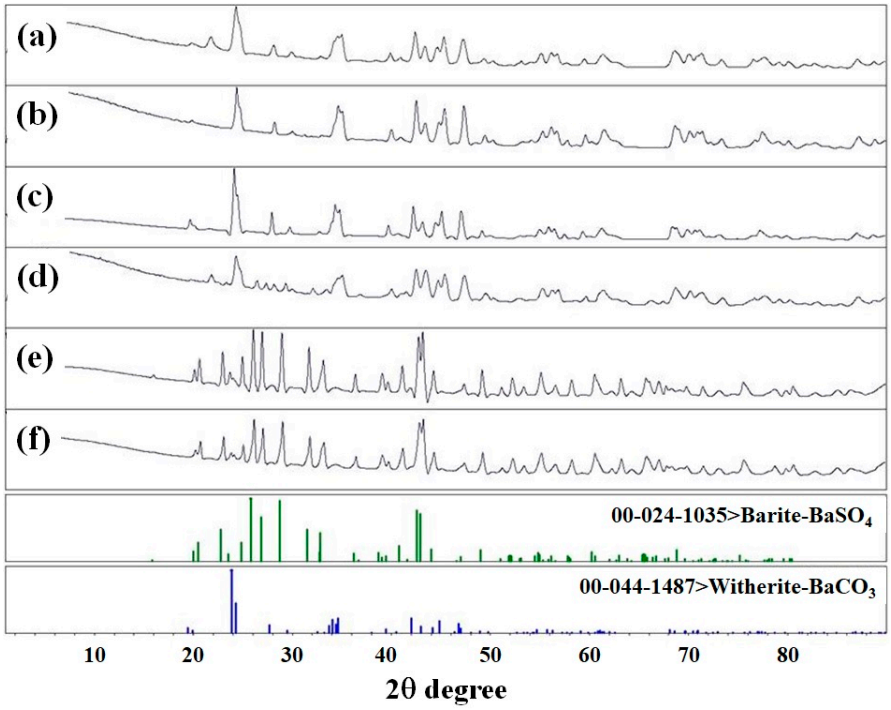

Figure 1. XRD pattern of before sulfate adsorption (**a**) PCL/Ba (50/50), (**b**) PCL/Ba (2.5/97.5), and (**c**) PCL/Ba (10/90), and after sulfate adsorption (**d**) PCL/Ba (50/50), (**e**) PCL/Ba (2.5/97.5), and (**f**) PCL/Ba (10/90).

Figure 2a–h shows SEM images of control $BaCO_3$ and PCL/Ba samples with different magnifications. Figure 2a,b represents control $BaCO_3$ with low and high magnification, respectively. The particle sizes ranged from a few hundred nanometers to microns in length. Elongated rod-shaped structures with hexagonal phases were observed. Figure 2c–h show SEM images of PCL/Ba samples before barium sulfate precipitation. $BaCO_3$ particles were dispersed without surface morphology changes in the polymer matrix. $BaCO_3$ particles aggregated with an increase in the amount of polymer in the PCL/Ba composite (Figure 2c), indicating less polymer content in the composites is better to effectively disperse $BaCO_3$ in the composites (Figure 2e,g). The control $BaCO_3$ crystals dispersed in PCL had elongated structures with hexagonal faces as seen in Figure 2d,f,h.

Figure 3a–f shows SEM images of PCL/Ba (50/50), (10/90), and (2.5/97.5) with lower and higher magnification after sulfate adsorption, respectively. Well-defined barium sulfate cubes were observed in all PCL/Ba composites. In a previous study [9], the formation of $BaSO_4$ with a cubic structure was reported after sulfate adsorption using $BaCO_3$. In addition to the formation of $BaSO_4$ cubes, the bulk morphology of PCL in PCL/Ba (50/50) sample was observed due to the high content of PCL in the sample. Interestingly, random sized $BaSO_4$ cubes were observed in the samples containing less $BaCO_3$. Based on these results, it could be hypothesized that more controlled and well-defined $BaSO_4$ crystals can be precipitated when the barium content of the PCL/Ba composite is lower. The reasoning behind such a trend has been explained by Kucher et al., who studied the influence of supersaturation and free lattice ion ratio on barium sulfate particle formation. While heterogeneous nucleation dominates crystal formation at lower supersaturation levels, it is substituted by homogeneous nucleation at higher levels of supersaturation. Homogeneous nucleation promotes the formation of smaller crystals up to about 100 nm in size as opposed to larger well-defined crystals at lower levels. Similarly, in the present study, well-defined crystals were observed in composites with lower barium content as compared to random, smaller crystals formed with higher levels of barium-containing composites [19].

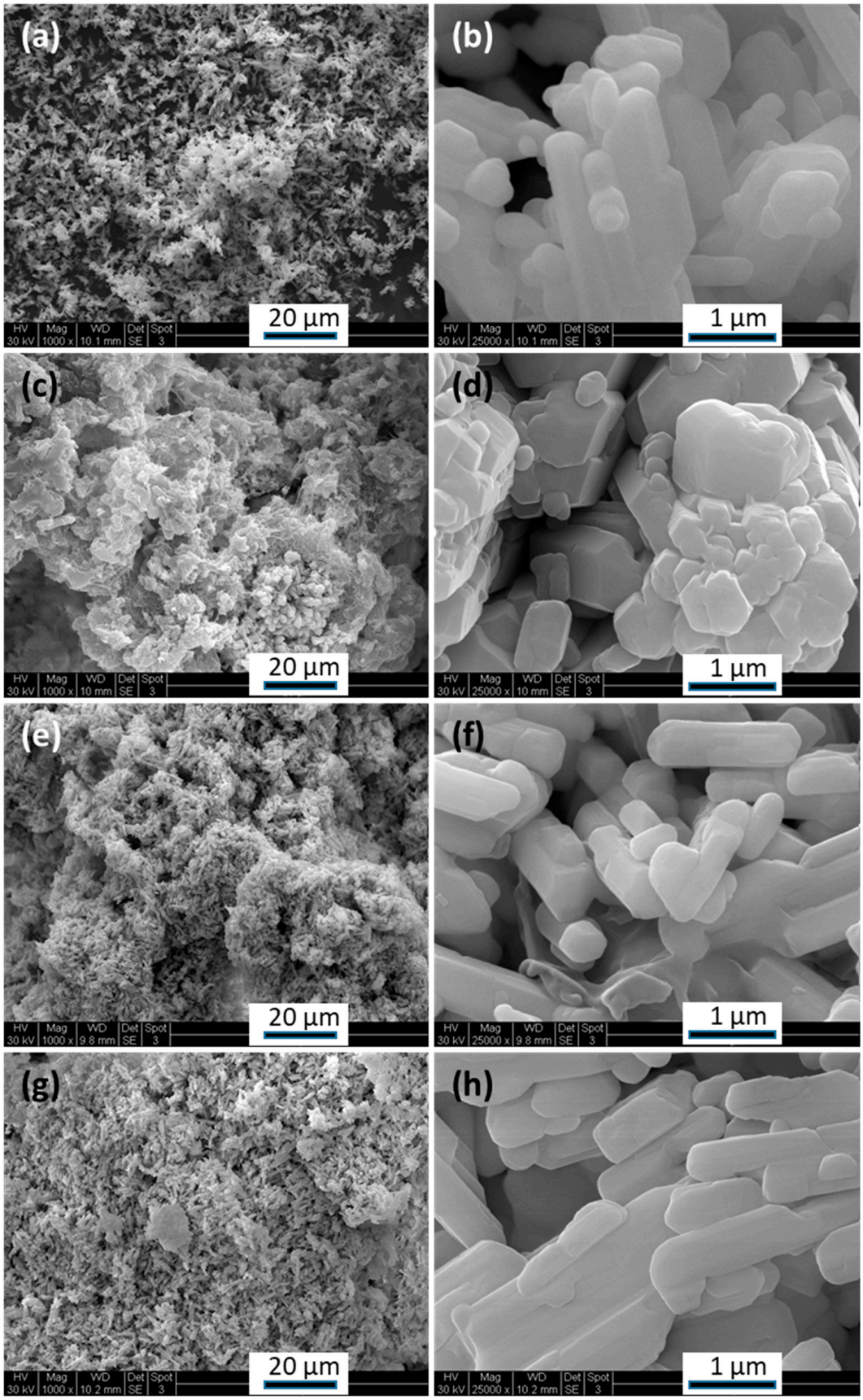

Figure 2. SEM images of control $BaCO_3$ (**a**) and (**b**), and PCL/Ba samples; (50/50) (**c**) and (**d**), (10/90) (**e**) and (**f**), and (2.5/97.5) (**g**) and (**h**) at low and high resolution.

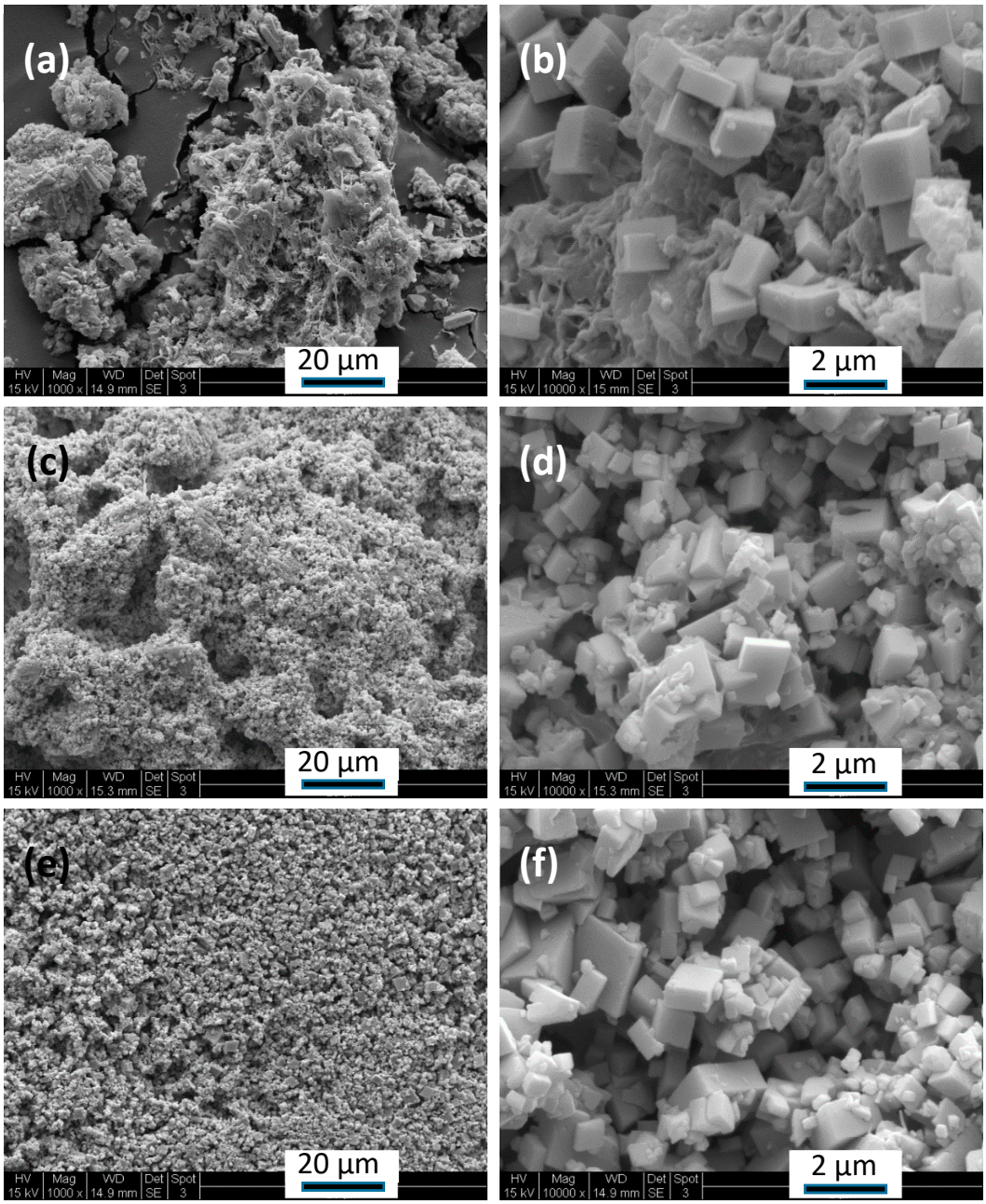

Figure 3. SEM Images after $BaSO_4$ precipitation; (**a**) and (**b**) PCL/Ba (50/50); (**c**) and (**d**) PCL/Ba (10/90), and (**e**) and (**f**) PCL/Ba (2.5/97.5) composites.

Figure 4a–f shows TEM images of PCL/Ba composites before and after sulfate adsorption. Before sulfate adsorption, elongated $BaCO_3$ was observed in all samples, as seen in Figure 2a–h. After sulfate removal, the transformation from a rod-shaped structure to the cubic structure was observed, which is in good agreement with the SEM images (Figure 3b,d,f). These results indicate the formation of $BaSO_4$ cubes after sulfate adsorption. However, the formation of the $BaSO_4$ cube with a uniform size was not observed in the PCL/Ba (50/50) sample. Due to the high content of PCL in the sample, $BaCO_3$ particles were capped with PCL as seen in Figure 4b. To confirm the formation of $BaSO_4$ after sulfate removal, HR-TEM analysis was performed in PCL/Ba (10/90) sample. Figure 5a,b shows the HR-TEM images of the PCL/Ba (10/90) sample after sulfate removal.

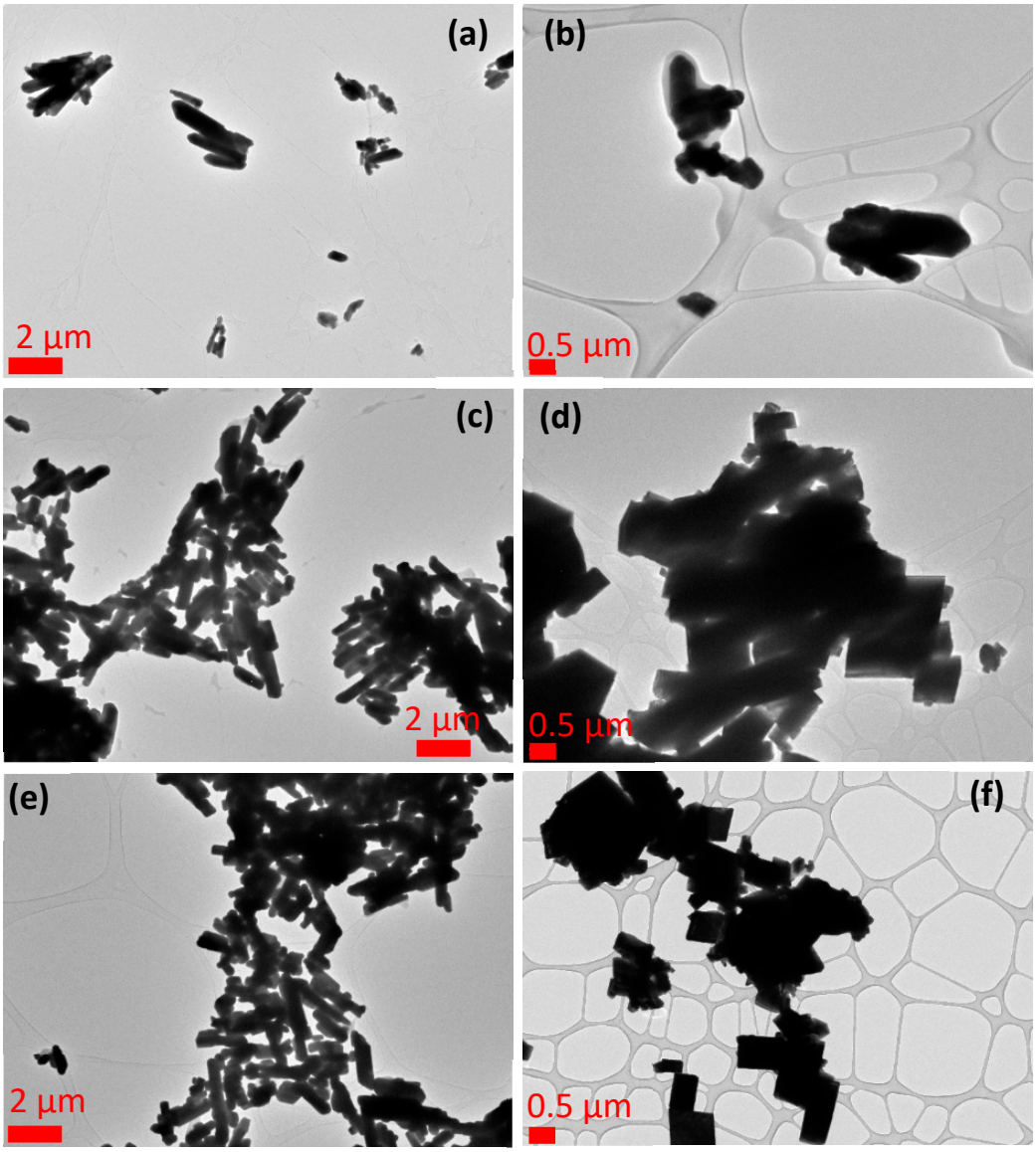

Figure 4. TEM Images before (**a**,**c**,**e**) and after (**b**,**d**,**f**) $BaSO_4$ precipitation; (**a**) and (**b**) PCL/Ba (50/50), (**c**) and (**d**) PCL/Ba (10/90), and (**e**) and (**f**) PCL/Ba (2.5/97.5).

As seen in Figure 5a, the lattice spacing of 0.210 and 0.312 nm corresponding to (212) and (121) plane of Barite, respectively, was measured, which indicates the formation of $BaSO_4$ after sulfate adsorption. In addition, the measured lattice spacing in the sample after NOM removal as sulfate was 0.211 nm corresponding to (212) plane of Barite, indicating the PCL/Ba sample effectively removes sulfate in water. These results are in good agreement with the results of XRD analysis, confirming the formation of $BaSO_4$ after sulfate adsorption.

Table 2 summarizes theoretical and experimental sulfate adsorption capacity of PCL/Ba samples obtained from various SST, conducted using different size columns and various PCL/Ba composites. The theoretical capacity of the media was determined by taking into account that, according to the chemical reaction, 1 mole of barium reacts with 1 mole of sulfate to form barium sulfate. Therefore, the barium content in the media determined using EDS was used to calculate the theoretical sulfate removal capacity of the media in mg/g. The results shown in Table 2 indicate that a lesser amount of polymer with a higher barium content in the composites helps improve the capacity of the media. The composite with lowest PCL (2.5%) and highest barium content (97.5%) was capable of achieving 72.4% of the theoretical capacity, as opposed to the PCL/Ba (50/50) which performed poorly.

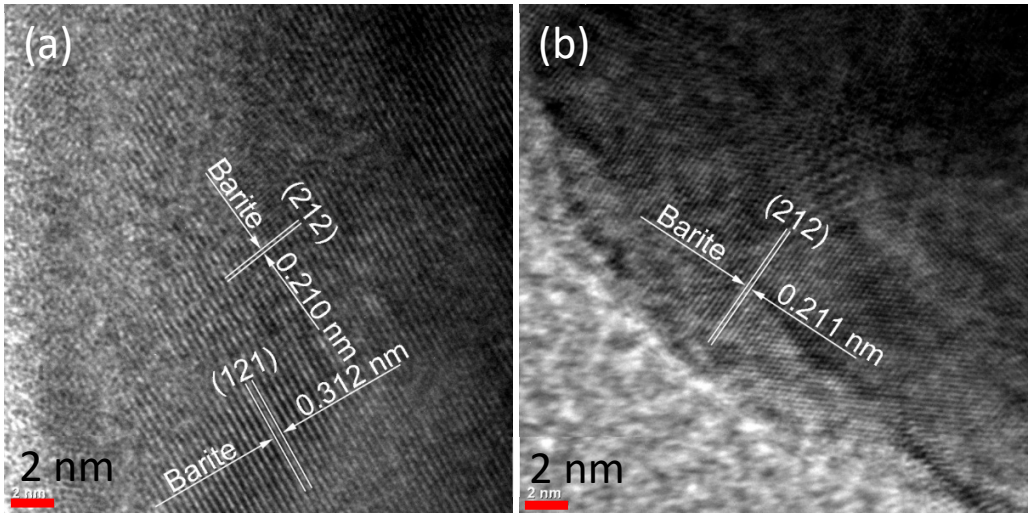

Figure 5. HR-TEM images of the PCL/Ba (10/90) sample after sulfate removal: (**a**) dissolved sulfate and (**b**) natural organic matter (NOM) as sulfate.

Table 2. Theoretical and experimental sulfate adsorption capacity of PCL/Ba samples obtained from a small-scale column test (SST).

Material	Theoretical (mg/g)	Experimental (mg/g)	Percent (%)
PCL/Ba (50/50); D = 1 cm	243.4	2.8	1.2
PCL/Ba (10/90); D = 1 cm	438.1	262.1	59.8
PCL/Ba (10/90); D = 2.25 cm	438.1	223.8	51.1
PCL/Ba (2.5/97.5); D = 2.25 cm	474.6	343.8	72.4

Thermogravimetric analysis was done on various $BaCO_3$ loaded polycaprolactone composites and these thermograms are shown in Figures 6 and 7. The control polycaprolactone has a broad decomposition temperature around 380 to 415 °C. The addition of $BaCO_3$ decreased the decomposition temperatures (see Figure 6). In addition, the decomposition temperatures are very sharp compared to pure polycaprolactone. The PCL/Ba (90/10) has a sharp decomposition temperature at around 335 °C, whereas PCL/Ba (50/50) has a decomposition temperature of 320 °C.

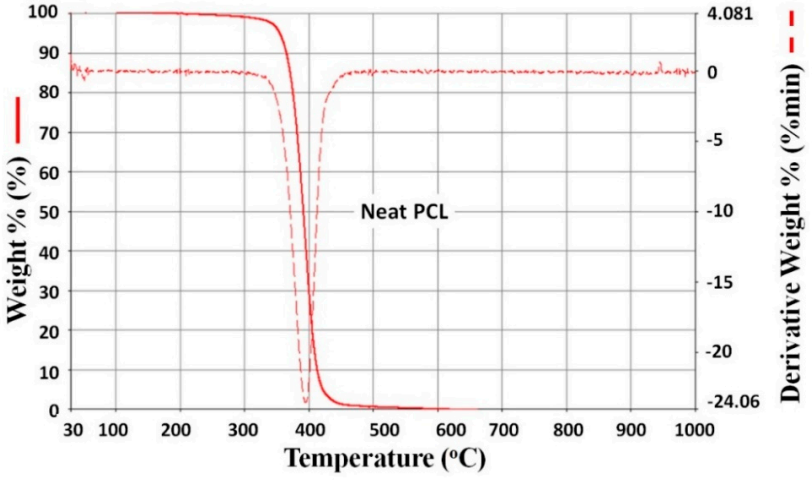

Figure 6. Thermogram of pure polycaprolactone polymer.

The increase in the quantity of $BaCO_3$ loaded in the polymer composite in turn accelerated the early decomposition temperatures. For example, PCL/Ba (30/70) has a broad decomposition temperature from 250 to 300 °C and PCL/Ba (10/90) has a broad decomposition temperature of 200 to 250 °C, which is much lower compared to PCL/Ba (90/10).

The drastic decrease in decomposition temperatures resulting from increasing $BaCO_3$ content is unclear and requires detailed mechanistic studies. Similar observations were reported by Liu et al., wherein higher $CaSO_4$ loading in polycaprolactone composites decreased decomposition temperatures [20]. Possible reasons for the abnormal decrease in temperature may have been due to poor recrystallization and weak bonding of polycaprolactone in the presence of $BaCO_3$. However, a different trend was observed by Lee et al. in the case of carbon nanotubes (CNT) dispersed polycaprolactone composites. Thermal stability increased even in the presence of a small amount of multi-walled CNT-Cl, which suggests the homogeneous dispersion in the composites CNT [21]. Trapped solvent decomposition may have also played a role in causing the abnormal decrease in temperature.

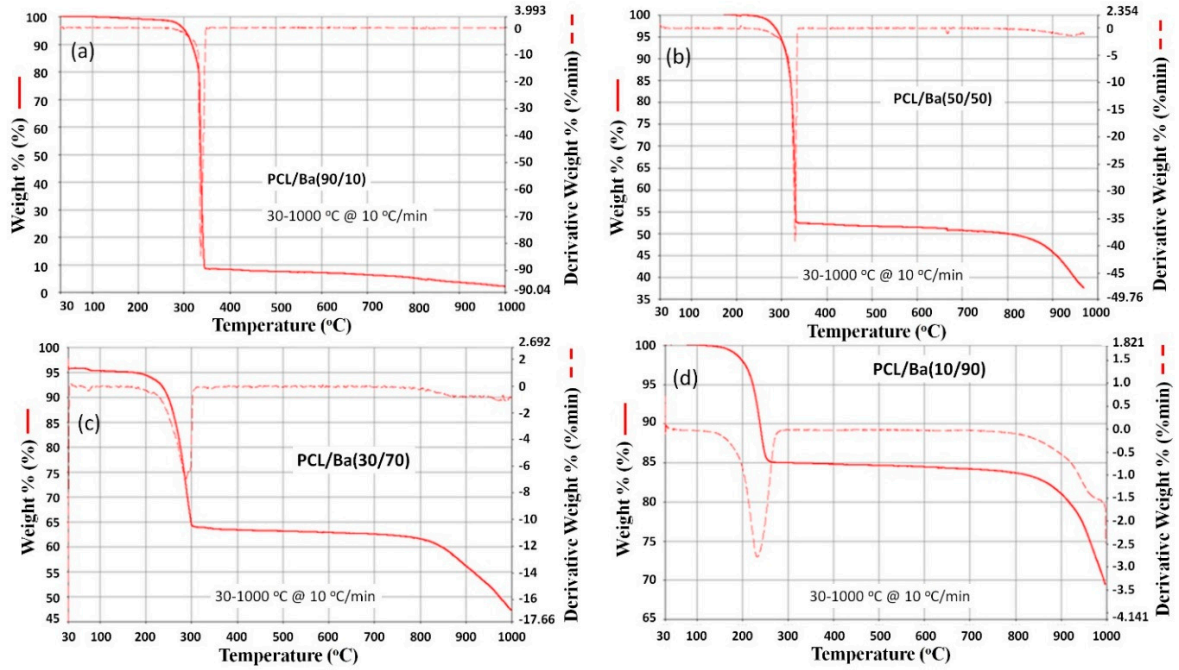

Figure 7. Thermograms of PCL/Ba composites: (**a**) 90/10, (**b**) 50/50, (**c**) 30/70, and (**d**) 10/90.

Figure 8 shows the sulfate removal of PCL/Ba composites with column tests. Symbols of white circles depict the influent sulfate concentration, which was kept constant at 1100 mg/L. There are two significant results shown in Figure 8. Firstly, the sulfate removal depends on the amount of polymer and barium in the composites. The sample, containing a small amount of polymer (and consequently a large amount of barium), demonstrated higher sulfate removal compared to other samples. In the case of the PCL/Ba (50/50) sample, the column is saturated earlier compared to other samples due to a lower barium content, while a similar sulfate removal pattern is observed for PCL/Ba (2.5/97.5) and (10/90) composites. The existence of such a direct proportionality between the efficiency of sulfate removal and the cation content of the media has been studied by other researchers [22]. Sulfate in the effluent was not detected for the first 10 minutes, while after this point it spiked to about 600 mg/L and maintained this level until about 4000 and 7000 min for PCL/Ba (2.5/97.5) and (10/90), respectively. Such a pattern in sulfate removal using PCL/Ba media can be explained by mass transfer principles. In the initial phase, barium available on the exterior of the packed column comes in contact with sulfate and quickly becomes saturated. After that, it takes a longer time for the sulfate molecules to access the barium molecules buried inside of the polymer matrix. Once all the barium molecules are

saturated with adsorbed sulfate, the media reaches complete saturation and is not capable of any further sulfate removal.

The wall effect was studied in the process by conducting experiments in smaller and larger diameter columns loaded with the same amount of PCL/Ba media. As seen in Figure 8, the friction was reduced significantly due to the wall surface when larger diameter columns were used. Although saturation in the larger diameter column (d = 2.25 cm) was achieved much quicker compared to the smaller diameter (d = 1.0 cm) column, the percentage of sulfate removal was higher in the smaller. Higher sulfate removal in the smaller column was the result of a longer retention time and hence better diffusion of sulfate molecules through the polymer matrix.

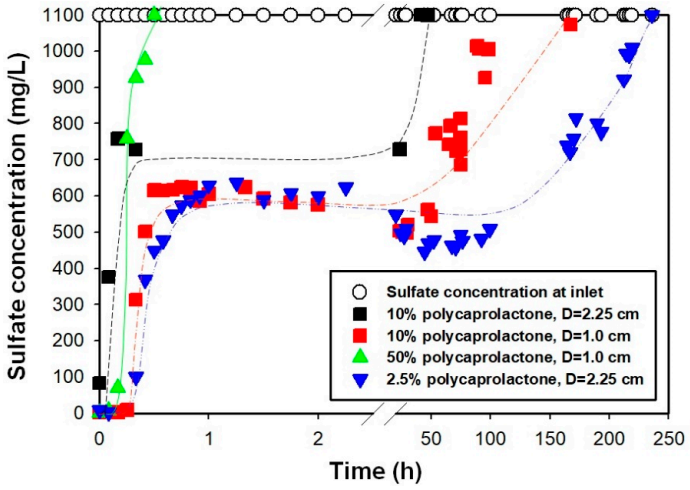

Figure 8. Comparison of remediation media for sulfate removal.

Figure 9 shows NOM removal as sulfate using PCL/Ba media. After passing sulfate containing NOM through the column for about 500 min, the PCL/Ba (10/90) media was able to remove more than 90% of the influent sulfate. A previous study on sulfate removal from wastes by precipitation by Beatti et al. [23] reported that only 61.4% of the influent sulfate was removed using the barium precipitation technique under a sulfate concentration of 80 g/L in the influent. In the present study, the effluent sulfate concentrations remained well below 30–50 mg/L for the first two hours except for an outlier seen at 1 hour, removing more than 90% of influent sulfate because lower sulfate concentration (328 mg/L) was fed into the column. Such promising results show that the media used in this study has a very high capacity to remove low concentrations of sulfate, and further studies are required in pilot scale to evaluate a long-term activity of these media.

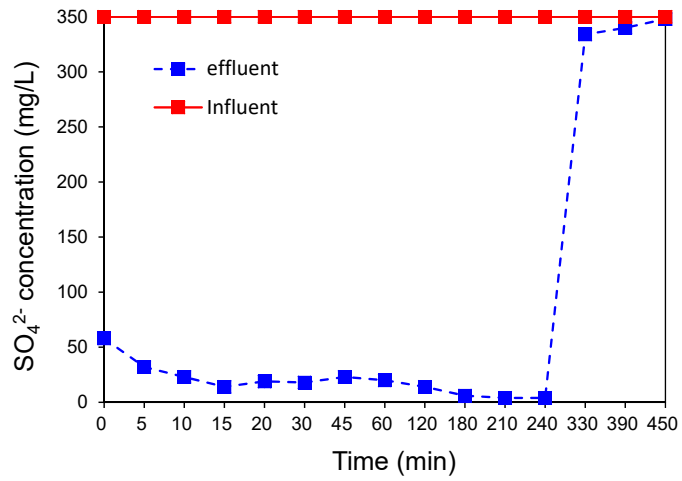

Figure 9. Sulfate concentration in NOM samples in influent and effluent of PCL/Ba (10/90) packed columns (Diameter: 2.25 cm).

Table 3 shows the cumulative capacity of the PCL/Ba (10/90) composite used to remove sulfate from NOM containing Ohio River water. After passing sulfate containing water through the column for 450 min, the polymer composite was saturated, indicating that all the accessible barium molecules were bound with sulfate molecules to form barium sulfate. From Table 3, it can be seen that PCL/Ba (10/90) exhibited a high capacity and removed more than 90% of the influent sulfate, and the cumulative capacity was calculated to be 175.8 mg/g.

Table 3. Cumulative capacity of PCL/Ba (10/90) composite in the presence of SO_4 and NOM (Influent Concentration of sulfate: 328 mg/L and Flow rate: 2.0 mL/min).

Elapsed Time (min)	Effluent Conc (mg/L)	Cumulative Feed Volume (mL)	Bed Volumes Fed (mL)	Delta Capacity of Media (mg/g)	Cumulative Capacity of Media (mg/g)
0	58	0	0	0.0	0.0
5	32	10	4	2.8	2.8
10	23	20	8	3.0	5.8
15	14	30	13	3.1	8.9
20	19	40	17	3.1	12.0
30	18	60	25	6.2	18.2
45	23	90	38	9.2	27.5
60	103	120	51	8.0	35.4
120	14	240	102	32.3	67.8
180	6	360	153	38.2	105.9
210	5	420	178	19.4	125.3
240	5	480	204	19.4	144.6
330	317	660	280	30.1	174.7
390	324	780	331	0.9	175.6
450	328	900	382	0.2	175.8

Figure 10 shows an SEM image of the PCL/Ba (10/90) sample after sulfate removal in the Ohio River water containing NOM. The SEM image demonstrates irregular shaped barium sulfate crystals with different sizes ranging from 200 nm to 1 µm were formed after sulfate removal in the Ohio River water, which is in contrast to the well-defined cubes formed in the presence of synthetic sulfate containing solutions as shown in Figures 3 and 4.

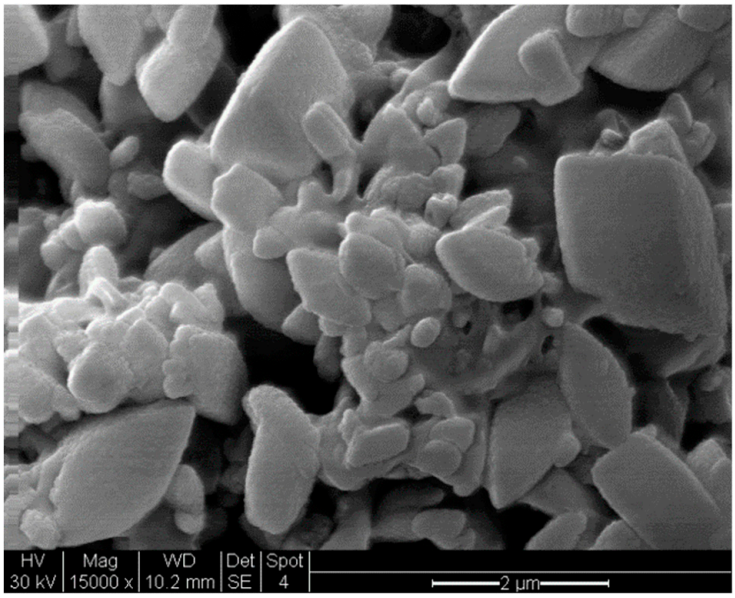

Figure 10. SEM image of $BaSO_4$ formed in the presence of sulfate and NOM from Ohio River water.

4. Conclusions

Use of barium encapsulated biodegradable polycaprolactone for environmental remediation of sulfate containing water was investigated. Various compositions of PCL/Ba composites were synthesized and tested by conducting SSTs to study the efficiency of sulfate removal. XRD, SEM, TEM, and HR-TEM analyses showed the formation of $BaSO_4$ after sulfate removal, indicating sulfate was effectively removed using PCL/Ba composites. The sulfate removal capacity of PCL/Ba media was dependent on the amount of barium in the composites and was proportional to the amount of barium in the media. It was observed that PCL/Ba (10/90) had the highest capacity and was effective for sulfate removal from NOM samples under these experimental conditions. The sulfate removal was higher in the small column due to a longer retention time for mass transfer compared to the large column. Moreover, the use of a biodegradable polymer for material synthesis helps to overcome the concern over plastic leaching into water supplies.

Author Contributions: Conceptualization, Methodology, Validation, Formal Analysis, Investigation, Writing-Original Draft Preparation, Writing-Review & Editing, and Visualization, C.H. and M.N.N.; Project Administration, M.N.N.

Funding: INHA University Research Grant (INHA-57849-1).

Acknowledgments: This work was supported by INHA University Research Grant (INHA-57849-1).

Conflicts of Interest: The authors declare no conflict of interest.

References

1. Choi, H.; Stathatos, E.; Dionysiou, D.D. Sol–gel preparation of mesoporous photocatalytic TiO_2 films and TiO_2/Al_2O_3 composite membranes for environmental applications. *Appl. Catal. B* **2006**, *63*, 60–67. [CrossRef]
2. Obare, S.O.; Meyer, G.J. Nanostructured Materials for Environmental Remediation of Organic Contaminants in Water. *J. Environ. Sci. Health A Tox. Hazard Subst. Environ. Eng.* **2004**, *39*, 2549–2582. [CrossRef] [PubMed]
3. Xu, J.; Bhattacharyya, D. Membrane-based bimetallic nanoparticles for environmental remediation: synthesis and reactive properties. *Environ. Prog.* **2005**, *24*, 358–366. [CrossRef]
4. Beatty, S.T.; Fischer, R.J.; Hagers, D.L.; Rosenberg, E. A Comparative Study of the Removal of Heavy Metal Ions from Water Using a Silica−Polyamine Composite and a Polystyrene Chelator Resin. *Ind. Eng. Chem. Res.* **1999**, *38*, 4402–4408. [CrossRef]
5. Khin, M.M.; Nair, A.S.; Babu, V.J.; Murugan, R.; Ramakrishna, S. A review on nanomaterials for environmental remediation. *Energy Environ. Sci.* **2012**, *5*, 8075–8109. [CrossRef]
6. WHO. Sulfate in Drinking-Water. 2004. Available online: http://www.who.int/water_sanitation_health/dwq/chemicals/sulfate.pdf (accessed on 5 December 2018).
7. Kaksonen, A.; Puhakka, J. Sulfate Reduction Based Bioprocesses for the Treatment of Acid Mine Drainage and the Recovery of Metals. *Eng. Life Sci.* **2007**, *7*, 541–564. [CrossRef]
8. Özdemir, M.; Çetisli, H. Sulfate Removal from Alunitic Kaolin by Chemical Method. *Ind. Eng. Chem. Res.* **2005**, *44*, 3213–3219. [CrossRef]
9. Nadagouda, M.N.; Pressman, J.; White, C.; Speth, T.F.; McCurry, D.L. Novel thermally stable poly(vinyl chloride) composites for sulfate removal. *J. Hazard. Mater.* **2011**, *188*, 19–25. [CrossRef]
10. Curran, C.M.; Tomson, M.B. Leaching of trace organics into water from five common plastics. *Ground Water Monit. Remediat.* **1983**, *3*, 68–71. [CrossRef]
11. Quevauviller, P.; Donard, O.; Bruchet, A. Leaching of organotin compounds from poly(vinyl chloride) (PVC) material. *Appl. Organomet. Chem.* **1991**, *5*, 125–129. [CrossRef]
12. Sadiki, A.D.; Williams, D.T. A study on organotin levels in Canadian drinking water distributed through PVC pipesa. *Chemosphere* **1999**, *38*, 1541–1548. [CrossRef]
13. Wu, W.; Roberts, R.S.; Chung, Y.C.; Ernst, W.R.; Havlicek, S.C. The extraction of organotin compounds from polyvinyl chloride pipe. *Arch. Environ. Contam. Toxicol.* **1989**, *18*, 839–843. [CrossRef]
14. Adriano, D.; Wenzel, W.; Vangronsveld, J.; Bolan, N.S. Role of assisted natural remediation in environmental cleanup. *Geoderma* **2004**, *122*, 121–142. [CrossRef]
15. Park, J.; Ye, M.; Park, K. Biodegradable Polymers for Microencapsulation of Drugs. *Molecules* **2005**, *10*, 146–161. [CrossRef] [PubMed]

16. Wu, K.J.; Wu, C.S.; Chang, J.S. Biodegradability and mechanical properties of polycaprolactone composites encapsulating phosphate-solubilizing bacterium *Bacillus sp*. PG01. *Process Biochem.* **2007**, *42*, 669–675. [CrossRef]
17. Sinha, V.; Bansal, K.; Kaushik, R.; Kumria, R.; Trehan, A. Poly-ϵ-caprolactone microspheres and nanospheres: An overview. *Int. J. Pharm.* **2004**, *278*, 1–23. [CrossRef] [PubMed]
18. Yang, Q.; Chen, L.; Shen, X.; Tan, Z. Preparation of Polycaprolactone Tissue Engineering Scaffolds by Improved Solvent Casting/Particulate Leaching Method. *J. Macromol. Sci. B* **2006**, *45*, 1171–1181. [CrossRef]
19. Kucher, M.; Babic, D.; Kind, M. Precipitation of barium sulfate: Experimental investigation about the influence of supersaturation and free lattice ion ratio on particle formation. *Chem. Eng. Process.* **2006**, *45*, 900–907. [CrossRef]
20. Liu, J.; Reni, L.; Wei, Q.; Wu, L.; Liu, S.; Wang, Y.; Li, G. Fabrication and characterization of polycaprolactone/calcium sulfate whisker composites. *Express Polym. Lett.* **2011**, *5*, 742–752. [CrossRef]
21. Lee, H.H.; Shin, U.S.; Jin, G.Z.; Kim, H.W. Highly Homogeneous Carbon Nanotube-Polycaprolactone Composites with Various and Controllable Concentrations of Ionically-Modified-MWCNTs. *Bull. Korean Chem. Soc.* **2011**, *32*, 157–161. [CrossRef]
22. Slingsby, R.; Pohl, C. Approaches to sample preparation for ion chromatography sulfate precipitation on barium-form ion exchangers. *J. Chromatogr. A* **1996**, *739*, 49–55. [CrossRef]
23. Benatti, C.T.; Tavares, C.R.G.; Lenzi, E. Sulfate removal from waste chemicals by precipitation. *J. Environ. Manag.* **2009**, *90*, 504–511. [CrossRef] [PubMed]